Improved Direct Torque Control for Sensorless Matrix Converter Drives with Constant Switching Frequency and Torque Ripple Reduction

Kyo-Beum Lee and Frede Blaabjerg

Abstract: In this paper, an improved direct torque control (DTC) method for sensorless matrix converter drives is proposed which enables to minimize torque ripple, to obtain unity input power factor, and to achieve good sensorless speed-control performance in the low speed operation, while maintaining constant switching frequency and fast torque dynamics. It is possible to combine the advantages of matrix converters with the advantages of the DTC strategy using space vector modulation and a flux deadbeat controller. To overcome the phase current distortion by the non-linearity of a matrix converter drive, the simple non-linearity compensation method using PQR power theory are presented in the proposed scheme. Experimental results are shown to illustrate the feasibility of the proposed strategy.

Keywords: DTC-SVM, deadbeat control, matrix converter, and sensorless induction motor drive.

1. INTRODUCTION

The induction motor drive fed by a matrix converter is superior to the conventional PWM-VS inverter because of the lack of bulky DC-link capacitors with limited life time, the bi-directional power flow capability, the sinusoidal input/output currents, and adjustable input power factor. Furthermore, because of a high integration capability and a higher reliability of the semiconductor device structures, the matrix converter topology is recommended for extreme temperatures and critical volume/weight applications. However, only a few of the practical matrix converters have been applied to induction motor drive system because the implementation of the switch devices in the matrix converter is difficult and modulation technique and commutation control are more complicated than the conventional PWM inverter [1-3].

The Direct Torque Control (DTC) scheme for matrix converter drives was initially presented in [4]. The generation of the voltage vectors required to implement the DTC of induction motors under the constraint of unity input power factor was allowed. However, the DTC scheme using a switching table has some drawbacks. Switching frequency varies according to the motor speed and the hysteresis bands of torque and flux, large torque ripple is generated in a low speed range because of small back EMF of the induction motor, and a high control sampling frequency is required to achieve good performance [5]. Although several methods to solve these problems have been presented [6-10], these methods are designed for a conventional inverter drive system. On the contrary, research results to solve these problems for matrix converter drives have not been reported in the literature.

Since the fundamental output voltage cannot be detected directly from the matrix converter output terminal in a matrix converter drive, the command voltage is usually used instead of the actual one. However, the commanded voltage does not agree with the actual fundamental output voltage due to non-linear characteristic of the matrix converter, such as commutation delay, turn-on and turn-off time of switching device, and on-state switching device voltage drop. In order to compensate this problem, especially important at low speed, the authors have made an attempt to compensate the non-linear matrix converter effects with current sign and off-line manners [11]. However, it is difficult to determine the current sign when the phase currents are closed to zero. If the current sign is misjudged, the non-linearity model of a matrix converter operates improperly. It is also difficult to compensate the non-linearity effects perfectly by off-line manners because the switching times and voltage drops of the power devices are varied with the operating conditions [12].

In this paper, a new DTC-SVM scheme using a flux deadbeat controller for sensorless matrix converter drives is presented, which enables to minimize torque

Manuscript received January 17, 2005; revised August 2, 2005; accepted November 3, 2005. Recommended by Editorial Board member Tae-Woong Yoon under the direction of Editor Keum-Shik Hong. This work was supported by the Danish Research Council (contract no. 274-05-0156).

Kyo-Beum Lee and Frede Blaabjerg are with the Institute of Energy Technology, Aalborg University, DK-9220 Aalborg East, Denmark (e-mails: {kyl, fbl}@iet.aau.dk).

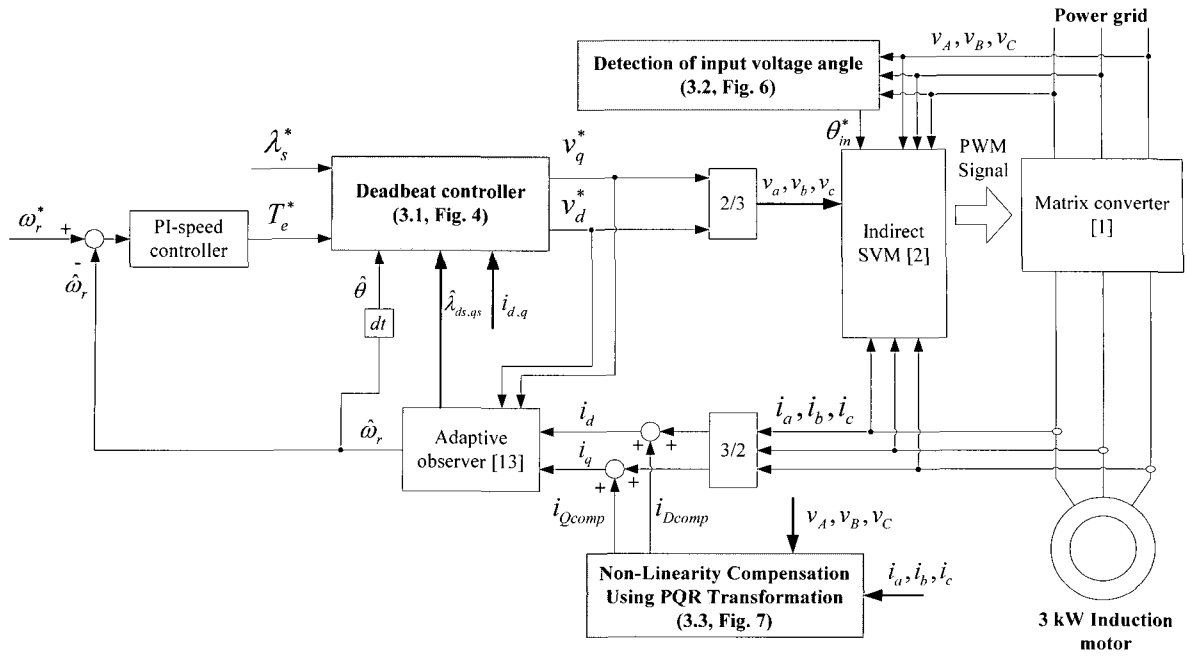

Fig. 1. The proposed sensorless modified DTC for matrix converter drives.

ripple and to obtain unity input power factor, while maintaining constant switching frequency. To improve the low-speed operation performance, an adaptive observer is employed for the estimation of the stator flux, the rotor speed, and the stator resistance [13]. In addition, a new on-line non-linearity compensation method for matrix converter drives using a PQR power theory [14] is proposed to realize high performance control. The proposed control scheme of the sensorless DTC for induction motor drives fed using a matrix converter is shown in Fig. 1, which consists of flux deadbeat controller, displacement angle calculator, indirect space vector modulation, an adaptive observer for speed and rotor flux estimation, and a simple non-linearity compensation for a matrix converter drive. Experimental results are presented to verify the effectiveness and feasibility of the proposed control system.

2. DTC FOR MATRIX CONVERTER

The principle of the DTC is briefly discussed and a torque, flux, and power factor control for matrix converter system are studied in this section. The DTC is a hysteresis torque and stator flux control that directly selects one of the six non-zero and two zero voltage vectors generated by a conventional two-level inverter in order to maintain the estimated stator flux and torque within the hysteresis bands. Fig. 2 shows a space vector representation of the conventional inverter output voltages.

An induction motor can be described in the stationary frame by the following flux and voltage equations.

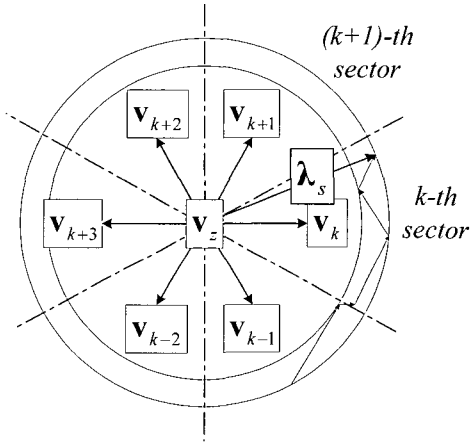

Fig. 2. The output voltage vectors in a conventional inverter system.

$$\boldsymbol{\lambda}_s = L_s \mathbf{i}_s + L_m \mathbf{i}_r, \qquad \boldsymbol{\lambda}_r = L_m \mathbf{i}_s + L_r \mathbf{i}_r, \tag{1}$$

$$\mathbf{v}_s = R_s \mathbf{i}_s + \frac{d}{dt}\boldsymbol{\lambda}_s, \qquad 0 = R_r \mathbf{i}_r + \frac{d}{dt}\boldsymbol{\lambda}_r - j\omega_r \boldsymbol{\lambda}_r, \tag{2}$$

where λ_s and λ_r are the stator and rotor flux vectors, $\mathbf{i}_s$ and $\mathbf{i}_r$ are the stator and rotor current vectors, $\mathbf{v}_s$ is the stator voltage vector, R_r is rotor resistance, L_s and L_r are stator and rotor self inductance, L_m is mutual inductance, and ω_r is the rotor speed.

From the induction motor equations (2) with the voltage drop across the stator resistance neglected, the relationship between the inverter output voltage vector and the variation of the stator flux can be expressed as

$$\Delta\boldsymbol{\lambda}_S = \left(\mathbf{v}_S - \mathbf{i}_S R_S\right) t_{sp} = \mathbf{e}_S t_{sp} \approx \mathbf{v}_S t_{sp}, \quad (3)$$

where $\mathbf{v}_s$ is the inverter output voltage vector, R_s is the stator resistance, $\mathbf{e}_s$ is the electromotive force vector, and t_{sp} is the sampling period.

(3) shows that an applied stator voltage vector produces a stator flux change. The amplitude of the stator flux change is proportional to the product of the applied voltage vector and the sampling period. The vectorial direction of the stator flux change coincides with the same as that of the selected voltage vector.

In general, in a symmetrical three-phase induction motor, the instantaneous electromagnetic torque is proportional to the cross-vectorial product of the stator flux vector and the stator-current vector [15].

$$T_e = \frac{3}{2} P \boldsymbol{\lambda}_S \times \mathbf{i}_S = \frac{3}{2} P |\boldsymbol{\lambda}_S| |\mathbf{i}_S| \sin\theta_{ss}, \quad (4)$$

where θ_{ss} is the angle between the stator flux and stator current vector, and P is the number of pole-pairs.

From (4), the electromagnetic torque can be quickly changed by controlling the stator flux vector, which, however, can be changed by using the appropriate stator voltages. If the modulus of the stator flux vector is kept constant and the angle is changed quickly, then the electromagnetic torque can be rapidly changed. It can be seen that there is direct stator and electromagnetic torque control achieved by using the appropriate stator voltages.

By using (1) and (4), the electromagnetic torque T_e can be rewritten as

$$T_e = \frac{3}{2} P \frac{L_m}{\sigma L_s L_r} \boldsymbol{\lambda}_r \times \boldsymbol{\lambda}_s = \frac{3}{2} P \frac{L_m}{\sigma L_s L_r} |\boldsymbol{\lambda}_r| |\boldsymbol{\lambda}_s| \sin\theta_{sr}, \quad (5)$$

where θ_{sr} is the angle between the stator and rotor flux vector and $\sigma = 1 - L_m^2 / L_s L_r$ is leakage coefficient.

By (1) and (2), the rotor flux can be written as a function of the stator flux as

$$\boldsymbol{\lambda}_r = \frac{L_m}{L_s} \frac{1}{1 + s\sigma\tau_r - j\omega_r \sigma\tau_r} \boldsymbol{\lambda}_s, \quad (6)$$

where $\tau_r = L_r / R_r$ is the rotor time constant.

(6) shows that the rotor flux tracks the stator flux with a delay of $\sigma\tau_r$. The rotor time constant τ_r of a standard squirrel-cage induction motor is large, thus the rotor flux changes only slowly compared to the stator flux. Therefore it can be assumed to be constant.

Assuming that the stator flux vector is in the kth sector, selection of the respective stator voltage vector is described in Fig. 2. The selection of $\mathbf{v}_{k+2}$ and $\mathbf{v}_{k+1}$ is able to increase the phase angle between the corresponding stator and rotor fluxes. As a consequence, the developed torque can be increased by the application of these voltages. It can be seen in Fig. 2 that the stator flux is increased by the selection of $\mathbf{v}_{k+1}$ and decreased by $\mathbf{v}_{k+2}$. The selection of $\mathbf{v}_z$, the stator flux vector λ_s comes to a stop that, since λ_r continues to move forward, causes a decrease in the angle θ_{sr} and then in the motor torque T_e. The resulting switching lookup table is shown in Table 1 [16].

Table 1. Switching look-up table for DTC.

$\boldsymbol{\lambda}_S$ in sector k		Torque	
		↑	↓
Flux	↑	$\mathbf{v}_{k+1}$	$\mathbf{v}_z$
	↓	$\mathbf{v}_{k+2}$	$\mathbf{v}_z$

Normally, the matrix converter is fed by a voltage source and, for this reason, the input terminal should not be short circuited, directly. On the other hand, the load has typically an inductive nature and, for this reason, an output phase must never be opened.

Defining the switching function of a single switch as

$$S_{Kj} = \begin{cases} 1, \text{ switch } S_{Kj} \text{ closed} \\ 0, \text{ switch } S_{Kj} \text{ open} \end{cases} \quad (7)$$

where $K=\{A, B, C\}$ is input phase and $j=\{a, b, c\}$ is output phase.

The constraints discussed above can be expressed by

$$S_{Aj} + S_{Bj} + S_{Cj} = 1 \quad (8)$$

with these restrictions, a 3×3 matrix converter has 27 possible switching states.

Let $m_{Kj}(t)$ be the duty cycle of switch S_{Kj}, defined as

$$m_{Kj}(t) = t_{Kj} / t_{sp}, \text{ where } 0 < m_{Kj} < 1. \quad (9)$$

The low-frequency transfer matrix converter is defined by

$$\mathbf{M}(t) = \begin{bmatrix} m_{Aa}(t) & m_{Ba}(t) & m_{Ca}(t) \\ m_{Ab}(t) & m_{Bb}(t) & m_{Cb}(t) \\ m_{Ac}(t) & m_{Bc}(t) & m_{Cc}(t) \end{bmatrix}. \quad (10)$$

The low-frequency component of the output phase voltage $\mathbf{v}_o$ is given by

$$\mathbf{v}_o(t) = \mathbf{M}(t) \cdot \mathbf{v}_i(t), \quad (11)$$

where $\mathbf{v}_o$ is the output voltage vector and $\mathbf{v}_i$ is the input voltage vector.

The low-frequency component of the input current $\mathbf{i}_i$ is

$$\mathbf{i}_i(t) = \mathbf{M}(t)^T \cdot \mathbf{i}_o(t), \quad (12)$$

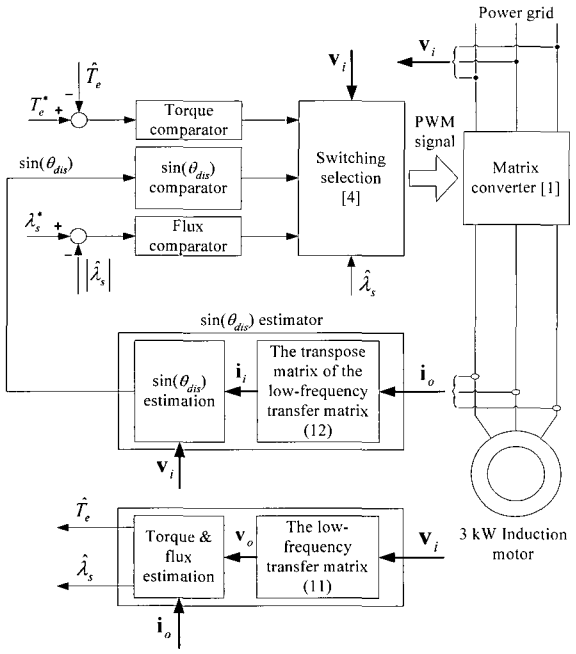

Fig. 3. The basic DTC for a matrix converter drive.

where $\mathbf{i}_i$ is the input current vector and $\mathbf{i}_o$ is the output current vector.

It appears that the matrix converter generates a higher number of output voltage vectors with respect to a conventional two-level inverter. In the DTC for matrix converter drives, the average value of the sine of the displacement angle θ_{dis} between the input line-to-neutral voltage vector and the corresponding input line current vector has been chosen as a third variable. The DTC for matrix converter drives selects the proper switching configuration at each sampling time, which allows the compensation of instantaneous errors in the flux magnitude, and torque, under the constraint of unity input power factor. The last requirement of the input side of the matrix converter is intrinsically satisfied if the average value of $\sin(\theta_{dis})$ is maintained close to zero. The average value of $\sin(\theta_{dis})$ is obtained by applying a low-pass filter to its instantaneous value. A schematic diagram of the DTC for a matrix converter drive is represented in Fig. 3.

The reference value of the torque and the stator flux magnitude are compared with the estimated value. The output of the hysteresis comparators, the stator flux, and input line-to-neutral voltage vector are the input to the switching selection algorithm [4]. The displacement estimator requires the knowledge of input voltages and output currents. However, only the input voltages and output currents are measured, while the other quantities are calculated on the basis of the low-frequency transfer matrix shown in Fig. 3.

3. AN IMPROVED DTC-SVM USING A DEADBEAT SCHEME AND SIMPLE NON-LINEARITY COMPENSATION

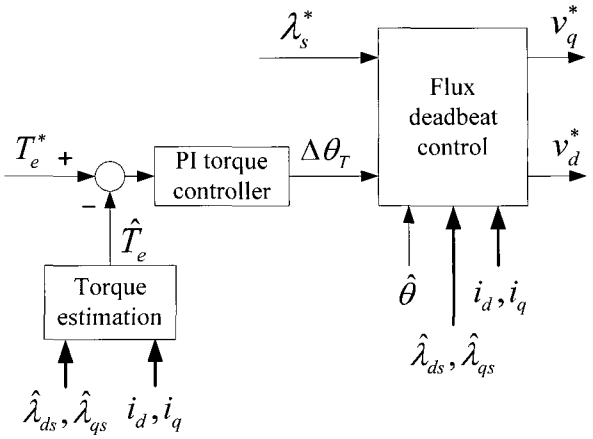

Fig. 4. Block diagram of the deadbeat controller.

The previous mentioned basic DTC method for matrix converter drives allows for the generation of the voltage vectors required to implement the DTC of the induction motor under the constraint of unity input power factor. However, the switching frequency varies according to the motor speed and the hysteresis bands of torque and flux, large torque ripple is generated in a low speed range because of small back EMF of an induction motor, and high control sampling time is required to achieve good performance [8]. In addition, the performance of the matrix converter is very dependent of the knowledge of the output voltage and therefore the matrix converter has to be modeled as a voltage source inverter [11]. To cope with these problems, a new modified DTC scheme is proposed. The proposed scheme is shown in Figs. 4-7, which consists of flux deadbeat controller, displacement angle calculation, and simple non-linearity compensation.

3.1. Deadbeat controller

The proposed DTC for matrix converter drives is presented in Fig. 1, and the internal structure of the torque and flux controller is shown in Fig. 4. In the proposed control system, a PI-torque controller and a flux deadbeat control scheme are used to determine the reference voltage vector for space vector modulation instead of torque and flux hysteresis controller for the switching vector table. The reference torque and the reference stator flux amplitude are delivered to the flux deadbeat controller. When the estimated torque is below the reference torque, the PI-torque controller generates the load angle increment to force the stator flux to rotate at higher speed, such that the instantaneous error between the reference torque and estimated torque is reduced to zero in each switching periods (see (3)). The stator voltage equation of induction motors in the stationary reference frame is given in (2). The reference values of d- and q- axis stator voltage are calculated taking

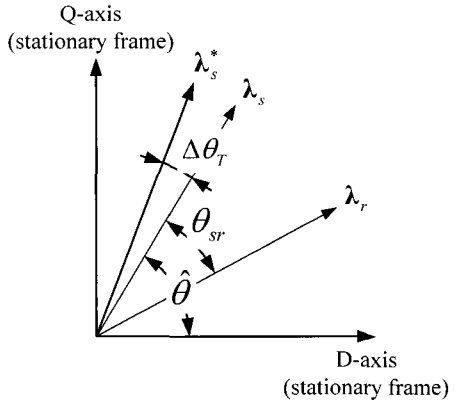

Fig. 5. Vector diagram of fluxes in induction motor.

into account the stator resistance, PI-torque controller output, estimated stator flux magnitude, actual stator currents, and rotor position.

The discrete form of (2) is

$$v_{ds,k} = \frac{\lambda_{ds,k} - \lambda_{ds,k-1}}{t_{sp}} + R_s i_{ds,k}, \tag{13}$$

$$v_{qs,k} = \frac{\lambda_{qs,k} - \lambda_{qs,k-1}}{t_{sp}} + R_s i_{qs,k}. \tag{14}$$

The d- and q- components of the reference flux can be written as (see Fig. 5)

$$\lambda^*_{ds,k} = \left|\boldsymbol{\lambda}^*_{s,k}\right| \cos\left(\hat{\theta}_k + \Delta\theta_{T,k}\right), \tag{15}$$

$$\lambda^*_{qs,k} = \left|\boldsymbol{\lambda}^*_{s,k}\right| \sin\left(\hat{\theta}_k + \Delta\theta_{T,k}\right). \tag{16}$$

Ideally, a deadbeat controller would establish zero flux error within one sampling period t_{sp}. The voltage vector $\mathbf{v}_{k+1}$ should be chosen in such a way that the resultant flux linkage in the next step will be

$$\boldsymbol{\lambda}_{s,k+1} = \boldsymbol{\lambda}^*_{s,k}. \tag{17}$$

It is necessary to impose the stator voltage at the (k+1)th sampling time, resulting in (13)-(17).

$$v_{ds,k+1} = \frac{\left|\boldsymbol{\lambda}^*_{s,k}\right| \cos\left(\hat{\theta} + \Delta\theta_T\right) - \left|\boldsymbol{\lambda}_{s,k}\right| \cos\left(\hat{\theta}\right)}{t_{sp}} + R_s i_{ds,k}, \tag{18}$$

$$v_{qs,k+1} = \frac{\left|\boldsymbol{\lambda}^*_{s,k}\right| \sin\left(\hat{\theta} + \Delta\theta_T\right) - \left|\boldsymbol{\lambda}_{s,k}\right| \sin\left(\hat{\theta}\right)}{t_{sp}} + R_s i_{qs,k}. \tag{19}$$

When the magnitude of the reference voltage vector $\mathbf{v}^*$ significantly exceeds the maximum realizable value, the inverter control is switched to the basic DTC block shown in Fig. 3. In this way, the drive combines advantages of the smooth steady-state operation and rapid response to the control commands.

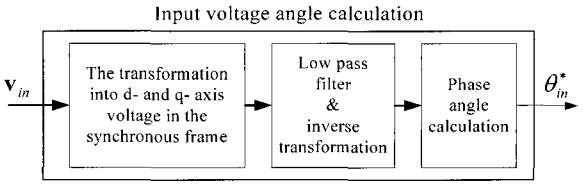

Fig. 6. The detection of the input voltage angle.

3.2. Detection of input voltage angle

To implement the ISVM (Indirect Space Vector Modulation), the input reference current vector is given by the input voltage vector for an instantaneous unity power factor. Under balanced conditions, the angular velocity as well as the magnitude of the input voltage vector is constant. In this situation the determination of the input current reference angle is quite straightforward. Unfortunately, with unbalanced supply voltages, the negative sequence component of the voltage causes variation in magnitude and angular velocity of the input voltage vector. A block diagram of the detection of input voltage angle is shown in Fig. 6. By using this simple method, a constant magnitude input voltage vector that rotates at a constant angular velocity can be made.

It can be seen from Fig. 4 and Fig. 6 that the presented DTC scheme retains the advantages of the conventional DTC, such as a very simple control structure without coordinate transformation, no current control loop, and also keeps unity input power factor. However, in (15), the stator resistance is still a key parameter in influencing the proposed DTC performance. The stator resistance is estimated under operation by an adaptive observer [16].

3.3. Non-linearity compensation using PQR transformation

The voltages due to the non-linearity of matrix converter drives cause the matrix converter output voltage distortion, results in the phase current distortion and torque ripple. The disturbance voltages is a function of a commutation delay, turn-on and turn-off time of the switching device, on-state switching device voltage drop and a current polarity [11]. However, the commutation delay, on-state voltage drop of the switching devices, and a current polarity are varying with the operating conditions. Since it is very difficult to measure the commutation delays and on-state voltage drops as well as to determine the current sign when the phase currents are closed to zero, it is not easy to compensate the non-linearity of matrix converter drives in an off-line manner [12].

To cope with these problems, a new on-line non-linearity compensation method using PQR transformation is proposed. The proposed scheme is shown in Fig. 7, which consists of a PQR transformation, a high-pass filter and a reference current control.

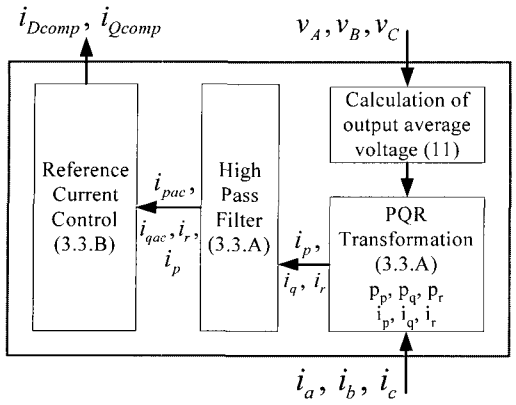

Fig. 7. The proposed non-linearity compensation method.

3.3.A Non-linearity of a matrix converter in PQR coordinates

The average components of the output voltages are calculated by (11). The reference voltages are defined as

$$\begin{bmatrix} v_o \\ v_\alpha \\ v_\beta \end{bmatrix} = \sqrt{\frac{2}{3}} \begin{bmatrix} 1/\sqrt{2} & 1/\sqrt{2} & 1/\sqrt{2} \\ 1 & -1/2 & -1/2 \\ 0 & \sqrt{3}/2 & -\sqrt{3}/2 \end{bmatrix} \begin{bmatrix} v_a \\ v_b \\ v_c \end{bmatrix} \text{ and}$$

$$\begin{bmatrix} v_p \\ v_q \\ v_r \end{bmatrix} = \frac{1}{v_{0\alpha\beta}} \begin{bmatrix} v_o & v_\alpha & v_\beta \\ 0 & -v_{o\alpha\beta} v_\beta / v_{\alpha\beta} & v_{o\alpha\beta} v_\alpha / v_{\alpha\beta} \\ v_{\alpha\beta} & -v_o v_\alpha / v_{\alpha\beta} & -v_o v_\beta / v_{\alpha\beta} \end{bmatrix} \begin{bmatrix} v_o \\ v_\alpha \\ v_\beta \end{bmatrix} = \begin{bmatrix} v_{\alpha\beta} \\ 0 \\ 0 \end{bmatrix}, \quad (20)$$

where $v_{\alpha\beta} = \sqrt{v_\alpha^2 + v_\beta^2}$ and $v_{o\alpha\beta} = \sqrt{v_o^2 + v_\alpha^2 + v_\beta^2}$.

The output currents in abc-coordinates can be transformed in PQR-coordinates as

$$\begin{bmatrix} i_o \\ i_d \\ i_q \end{bmatrix} = \begin{bmatrix} 1/\sqrt{2} & 1/\sqrt{2} & 1/\sqrt{2} \\ 1 & -1/2 & -1/2 \\ 0 & \sqrt{3}/2 & -\sqrt{3}/2 \end{bmatrix} \begin{bmatrix} i_a \\ i_b \\ i_c \end{bmatrix} \text{ and}$$

$$\begin{bmatrix} i_p \\ i_q \\ i_r \end{bmatrix} = \sqrt{\frac{2}{3}} \frac{1}{v_{0\alpha\beta}} \begin{bmatrix} v_o & v_\alpha & v_\beta \\ 0 & -v_{o\alpha\beta} v_\beta / v_{\alpha\beta} & v_{o\alpha\beta} v_\alpha / v_{\alpha\beta} \\ v_{\alpha\beta} & -v_o v_\alpha / v_{\alpha\beta} & -v_o v_\beta / v_{\alpha\beta} \end{bmatrix} \begin{bmatrix} i_o \\ i_d \\ i_q \end{bmatrix}. \quad (21)$$

The instantaneous real and imaginary powers can be expressed as

$$\begin{bmatrix} p \\ q_q \\ q_r \end{bmatrix} = \begin{bmatrix} v_p i_p \\ -v_p i_r \\ v_p i_q \end{bmatrix}, \quad (22)$$

where p is the instantaneous real power, q_q is the q axis instantaneous imaginary power, and q_r is the r axis instantaneous imaginary power.

The three instantaneous powers are linearly independent of each other. Thus, the three current components can be controlled independently by compensating the three instantaneous powers

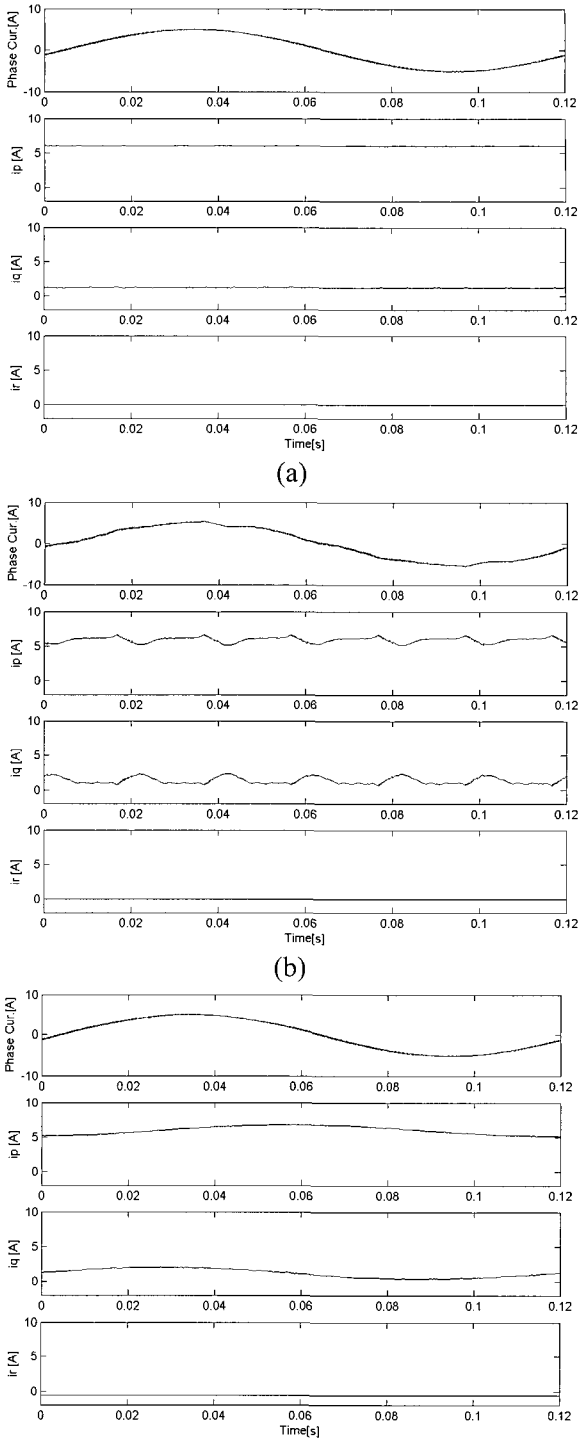

Fig. 8. Output current representation in PQR coordinates; From top, output phase current, p-, q-, and r-axis current (a) With an ideal matrix converter model, (b) With a practical matrix converter model, and (c) With an ideal matrix converter model and unbalanced current sensing.

respectively.

Fig. 8 shows some cases of the three-phase currents in PQR coordinates. In Fig. 8(a) the phase currents are

sinusoidal with an ideal matrix converter model. Thus i_r is zero, and i_p and i_q comprise only a dc component. In Fig. 8(b) the phase currents are distorted by the non-linearity of a matrix converter. There is no zero-sequence component in the sensed currents, so i_r is zero. The i_p and i_q contain an ac component. In Fig. 8(c) the phase current is sinusoidal but unbalanced sensing. Here the sum of the three-phase currents in a-b-c coordinates is not zero. Thus i_r has a non-zero dc value since it is directly related with the zero sequence component of three-phase currents. Then i_p and i_q contain not only a dc component but also an ac component.

As it is shown in the simulation results (Fig. 8), the r-axis current i_r is mainly related with the neutral-line current. If the matrix converter currents are balanced and sinusoidal, the i_p and i_q comprise only the dc component and i_r is zero. When the currents are unbalanced and distorted by the non-linearity of matrix converter, the unbalanced and harmonic component of the current exists in the i_p, i_q, and i_r. To eliminate these unbalanced and distorted currents due to current sensing unbalance and distortion by non-linearity of matrix converter drives, a reference current control method can be introduced. To make the compensation currents, a simple first order high-pass filter is used to separate the calculated variables into the ac and dc components. The classified ac and dc components are used to calculate the compensation current for the current controller.

3.3.B Reference current control

The reference current control can control the system currents to be three-phase sinusoidal balanced in any circuit conditions. The output phase currents, i_{as}, i_{bs}, and i_{cs} are transformed to PQR coordinates by the PQR transformation as shown in (21), resulting in i_p, i_q, and i_r. The i_p consists of an ac component, i_{pac} and a dc component, i_{pdc}. The i_q also consists of an ac component, i_{qac} and a dc component, i_{qdc}. The ac components, i_{pac} and i_{qac} are related with non-linear conditions such as the harmonics. The i_r represents the zero-sequence component of the output currents. Therefore to get the output currents symmetrical and sinusoidal, the currents, i_r must be compensated to zero and the current, i_p and i_q have to be controlled to a dc value.

The compensation currents can be represented as

$$\begin{aligned} i_{pcomp} &= i_{pac}, \\ i_{qcomp} &= i_{qac}, \\ i_{rcomp} &= i_r + \frac{v_o}{v_{\alpha\beta}} i_p. \end{aligned} \tag{23}$$

The i_{pcomp} is compensated for the p-axis, and the i_{qcomp}, i_{rcomp} are compensated for the q-axis and r-axis, respectively. The compensation currents in PQR coordinates, i_{pcomp}, i_{qcomp}, and i_{rcomp} are inversely transformed to d- and q- axis currents in the stationary reference frame by the inverse transformation of (21).

$$\begin{bmatrix} i_{Dcomp} \\ i_{Qcomp} \end{bmatrix} = \sqrt{\frac{3}{2}} \frac{1}{v_{0\alpha\beta}} \begin{bmatrix} v_\alpha & -v_{o\alpha\beta} v_\beta / v_{\alpha\beta} & -v_o v_\alpha / v_{\alpha\beta} \\ v_\beta & v_{o\alpha\beta} v_\alpha / v_{\alpha\beta} & -v_o v_\beta / v_{\alpha\beta} \end{bmatrix} \begin{bmatrix} i_{pcomp} \\ i_{qcomp} \\ i_{rcomp} \end{bmatrix} \tag{24}$$

The proposed compensation scheme is simple and calculating the compensation currents, i_{Dcomp} and i_{Qcomp} instantaneously in the stationary d-, q-frame. Each control variables can be controlled independently.

4. EXPERIMENTS

To confirm the validity of the proposed control algorithm, experiments are carried out. The system consists of a 3-phase, 380 V, 50 Hz, 4-pole, 3 kW induction motor and a power circuit with a matrix converter. The induction motor has the following parameter values: R_s=1.79 Ω, R_r=1.8 Ω, L_s=167 mH, L_r=174.4 mH, and L_m=160 mH. A dual controller system consisting of a 32-bit DSP (ADSP 21062) and

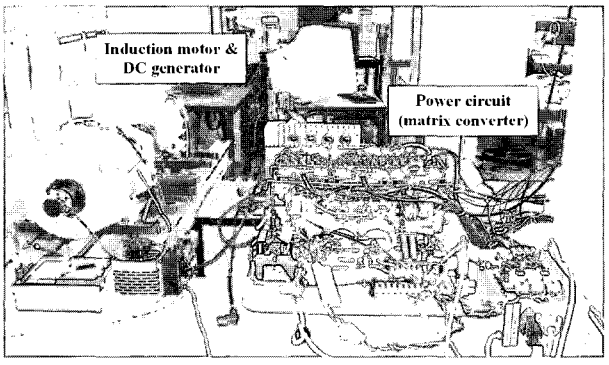

(a)

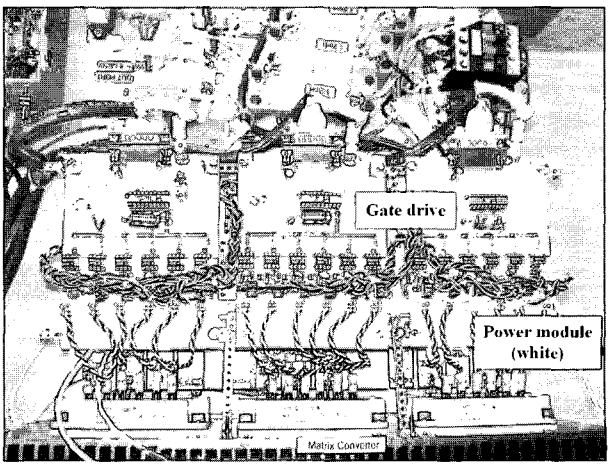

(b)

Fig. 9. Experimental set (a) total system and (b) matrix converter power circuit.

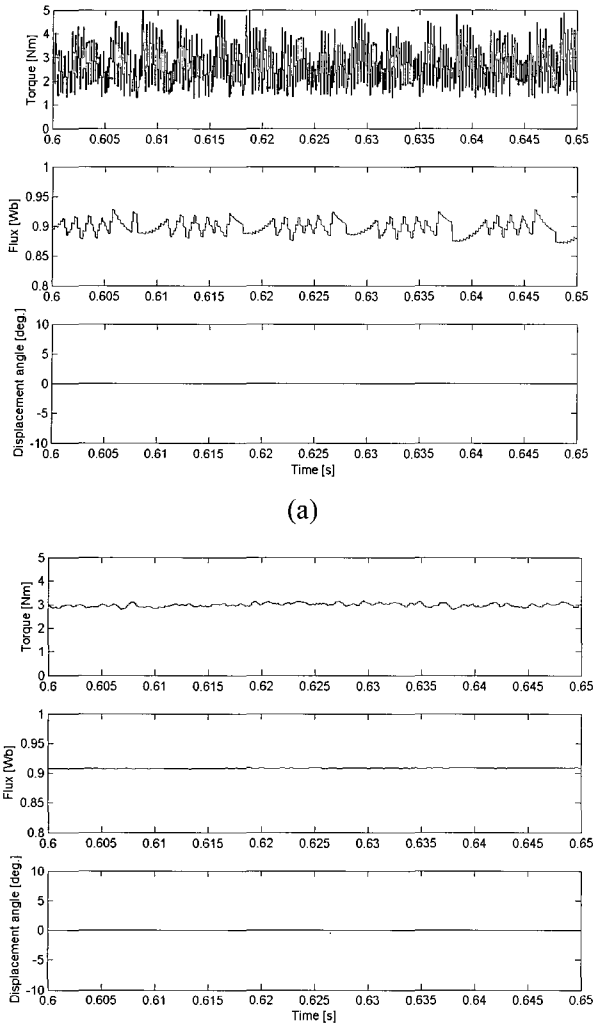

Fig. 10. Torque, flux, input power factor control at 500 rpm with 50 % of rated load: (a) Basic DTC and (b) Proposed DTC-SVM (estimated torque, flux and displacement angle).

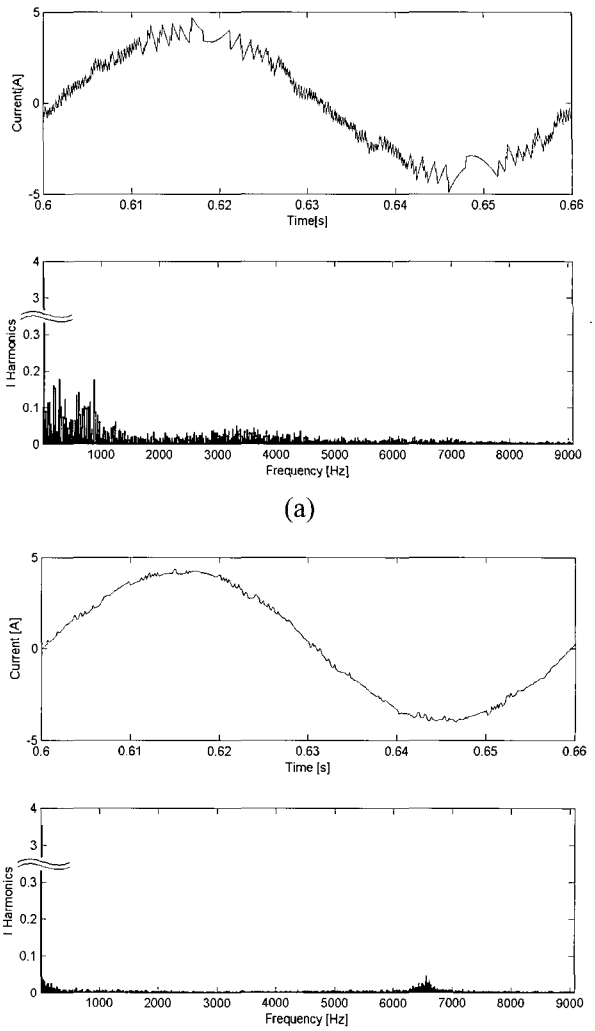

Fig. 11. Phase current in time and frequency domain at 500 rpm with 50 % of rated load: (a) Basic DTC, (b) Proposed DTC-SVM (phase current and harmonic spectrum).

a 16-bit microcontroller (80C167), in conjunction with a 12-bit A/D converter board is used to control the matrix converter based induction motor drive. In the experiments, the sampling period is 90 μs for the hysteresis-band based DTC and 150 μs for the modified DTC using SVM and flux deadbeat control. The modulation is using a double-sided SVM algorithm with minimized number of commutations and the commutation of the bi-directional switches was performed in a four-step way depending on the output current sign [17].

Fig. 9(a) shows the overall experimental setup. The matrix converter is feeding a 3 kW induction motor, which is mechanically coupled with a DC machine. The excitation of the DC machine is connected to an auto-transformer, via a diode rectifier, which provides variable excitation current, when needed. Fig. 9(b) shows the power part of the experimental setup. The printed circuit boards (PCB's) on top of each power module contain the gate drives.

Fig. 10(a) and (b) show the experimental results of the steady state performance of the basic DTC and the proposed improved DTC at 500 rpm. The torque and flux ripple of the basic DTC are 2.5 Nm and 0.05 Wb, respectively. However, the torque and flux ripple of the proposed DTC is almost zero. It is seen from this result that the torque and flux ripple are reduced drastically by the proposed algorithm.

The steady state phase current and their harmonic spectrums are compared in Fig. 11(a) and (b). From Fig. 11(a), a high distortion in the current can be observed and low order harmonics scattered from the fundamental to 4 kHz, which are not desirable. The current waveform of the proposed DTC in Fig. 11(b) is smoother than that of the basic DTC and the dominant harmonics are around 6.5 kHz which is

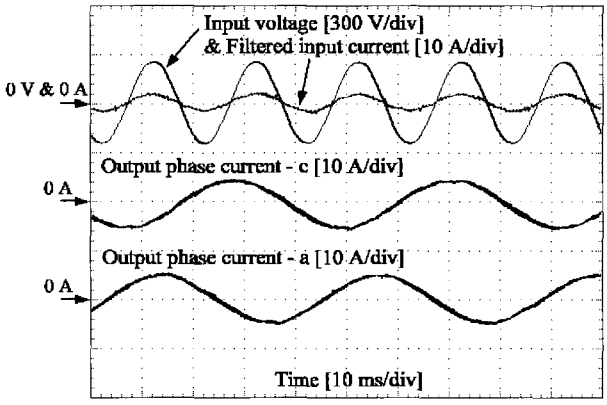

Fig. 12. Filtered input current, input line-to-neutral voltage, output phase currents of the proposed improved DTC-SVM at 700 rpm with 20 % of rated load.

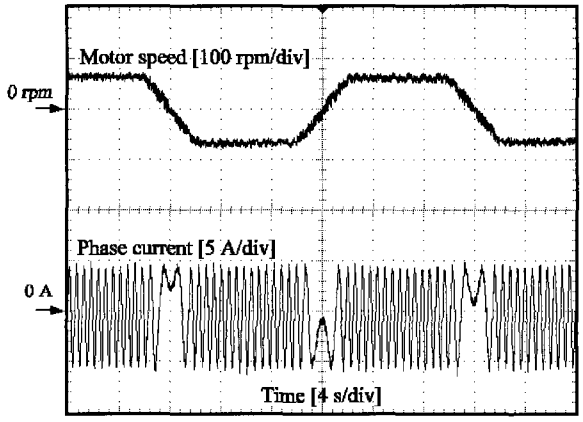

Fig. 13. Speed dynamic of the proposed DTC speed sensorless drive.

determined by the SVM sampling period.

Fig. 12 shows the filtered input line current and the corresponding line-to-neutral voltage. As it can be seen, the line current is in phase with the voltage, confirming the validity of the control scheme which allow unity input power factor operation.

Fig. 13 demonstrates the speed dynamic of the proposed DTC scheme in the forward and reverse operation. Fig. 13 shows the speed response for a ramp-speed reference with a slope 150 rpm/s. It is noted here that a smooth and stable zero crossing of the speed is obtained.

Fig. 14 shows the steady state characteristics of the speed and the phase current at 50 rpm. The nonlinearities cause undesired speed pulsations of about six times the electrical frequency and the phase current is not pure sinusoidal without nonlinearities compensation as shown in Fig. 14(a). However, in the proposed DTC with a simple compensation scheme, the speed ripple and the distortion in the phase current waveform are remarkably reduced as shown in Fig. 14(b).

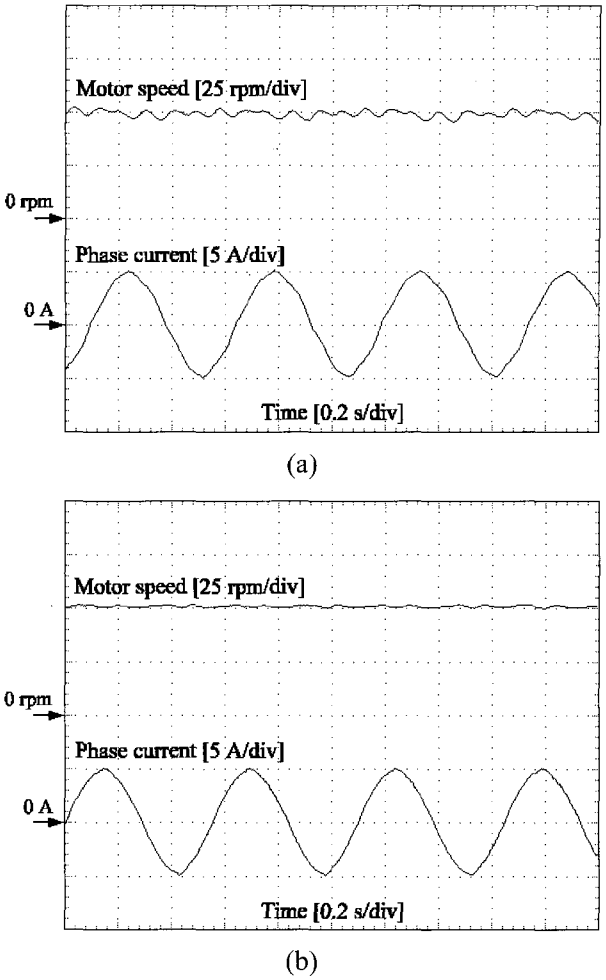

Fig. 14. Speed sensorless control at 50 rpm with 70 % of rated load ; speed and phase current (a) without non-linearity compensation, (b) with non-linearity compensation.

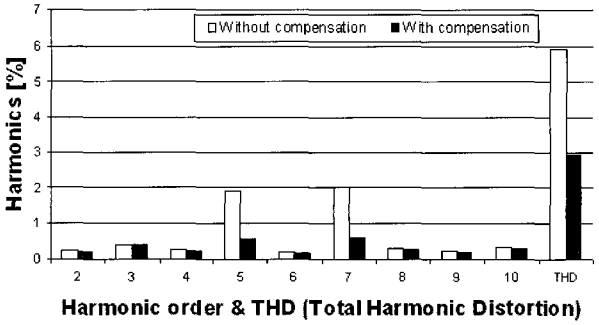

Fig. 15. Comparison of output current harmonics at 100 rpm.

Fig. 15 shows the experimental results with and without the proposed compensation method. The motor is also operated at 100 rpm. It can be seen from Fig. 15 that the current pulsations and their 5th and 7th harmonics are reduced with the proposed compensation method using the PQR transformation technique.

5. CONCLUSIONS

In order to realize high performance control of induction motor drives fed by a matrix converter, a new DTC method for sensorless matrix converter drives have been proposed in this paper. The proposed method using SVM, flux deadbeat controller with simple non-linearity compensation using PQR power theory enables to minimize current and torque ripple, to obtain unity input power factor, and to achieve good sensorless speed-control performance in the low speed operation, while maintaining constant switching frequency and torque dynamic response. It can be concluded from the experimental results that torque, flux, input power factor, and speed control performance are improved with the proposed improved DTC.

REFERENCES

[1] M. P. Kazmierkowski, R. Krishnan, and F. Blaabjerg, *Control in Power Electronics - Selected Problems*, Academic press, ISBN 0-12-402772-5, Ch. 3, 2002.

[2] P. W. Wheeler, J. Rodriguez, J. C. Clare, L. Empringham, and A. Weinstein, "Matrix converter: A technology review," *IEEE Trans. on Industrial Electronics*, vol. 49, pp. 276-288, Apr. 2002.

[3] L. Huber and D. Borojevic, "Space vector modulated three-phase to three-phase matrix converter with input power factor correction," *IEEE Trans. on Industry Applications*, vol. 31, pp. 1234-1246, Nov./Dec. 1995.

[4] D. Casadei, G. Serra, and A. Tani, "The use of matrix converters in direct torque control of induction machines," *IEEE Trans. on Industrial Electronics*, vol. 48, pp. 1057-1064, Dec. 2001.

[5] K. B. Lee, J. H. Song, I. Choy, and J. Y. Yoo, "Torque ripple reduction in DTC of induction motor driven by three-level inverter with low switching frequency," *IEEE Trans. on Power Electronics*, vol. 17, no. 2, pp. 255-264, Mar. 2002.

[6] L. Tang, L. Zhong, M. F. Rahman, Y. Hu, "A novel direct torque controlled interior permanent magnet synchronous machine drive with low ripple in flux and torque and fixed switching frequency," *IEEE Trans. on Power Electronics*, vol. 19, no. 2, pp. 346-354, Mar. 2004.

[7] M. Fu and L. Xu, "A sensorless direct torque control technique for permanent magnet synchronous motors," *Proc. of IEEE PESC99*, pp. 159-164, 1999.

[8] C. Lascu, I. Boldea, and F. Blaabjerg, "Variable structure direct torque control-A class of fast and robust controllers for induction machine drives," *IEEE Trans. on Industrial Electronics*, vol. 51, no. 4, pp. 785-792, Aug. 2004.

[9] B. H. Kenny and R. D. Lorenz, "Stator- and rotor-flux-based deadbeat direct torque control of induction machines," *IEEE Trans. on Industry Applications*, vol. 39, no. 4, pp. 1093-1101, Jul./Aug. 2003.

[10] Y. S. Lai and J. H. Chen, "A New approach to direct torque control of induction motor drives for constant inverter switching frequency and torque ripple reduction," *IEEE Trans. on Energy Conversion*, vol. 16, no. 3, pp. 220-227, Sept. 2001.

[11] K. B. Lee and F. Blaabjerg, "Performance improvement of sensorless vector control for induction motor drives fed by matrix converter using nonlinear model and disturbance observer," *Proc. of IEEE PESC04*, pp. 1341-1347, 2004.

[12] N. Urasaki, T. Senjyu, K. Uezato, and T. Funabashi, "A dead-time compensation strategy for permanent magnet synchronous motor drive suppressing current distortion," *Proc. of IEEE IECON03*, pp. 1255-1260, 2003.

[13] G. S. Lee, D. H. Lee, T. W. Yoon, K. B. Lee, J. H. Song, and I. Choy, "Speed and flux estimation for an induction motor using a parameter estimation technique," *International Journal of Control, Automation, and Systems*, vol. 3, no. 1, pp. 79-86, Mar. 2005.

[14] H. Kim, F. Blaabjerg, B. Bak-Jensen, and J. Choi, "Instantaneous power compensation in three-phase systems by using p-q-r theory," *IEEE Trans. on Power Electronics*, vol. 17, no. 5, pp. 701-710, Sept. 2002.

[15] P. Vas, *Sensorless Vector and Direct Torque Control*, Oxford University Press, ISBN 1-19-856465-1, 1998.

[16] K. B. Lee, J. H. Song, I. Choy, and J. Y. Yoo, "Improvement of low-speed operation performance of DTC for three-level inverter-fed induction motors," *IEEE Trans. on Industrial Electronics*, vol. 48, no. 5, pp. 1006-1014, Oct. 2001.

[17] P. Nielsen, F. Blaabjerg, and J. K. Pedersen, "New protection issues of a matrix converter: Design considerations for adjustable-speed drives," *IEEE Trans. on Industry Applications*, vol. 35, no. 5, pp. 1150-1161, Sept./Oct. 1999.

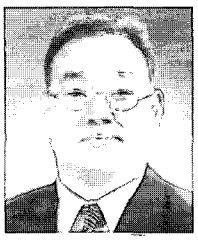

Kyo-Beum Lee received the B.S. and M.S. degrees in Electrical and Electronic Engineering from Ajou University, Suwon, Korea, in 1997 and 1999, respectively. He received the Ph.D. degree in Electrical Engineering from Korea University, Seoul, Korea in 2003. From 2003 to 2004, he was with the Research Institute for Information and Communication Technology as a Senior Researcher in Korea University. In 2004, he joined the Institute of Energy Technology, Aalborg University, Aalborg, Denmark. He received the best paper award at the 30th Annual Conference of the IEEE Industrial Electronics Society 2004 (IECON '04). His research interests include electric machine drives and power electronics.

Frede Blaabjerg received the M.Sc.EE. and Ph.D. degrees from Aalborg University, Aalborg, Denmark in 1987 and 1995, respectively. He was employed at ABB-Scandia, Randers, from 1987 to 1988. He became an Assistant Professor in 1992 at Aalborg University, an Associate Professor in 1996 and full professor in Power Electronics and Drives the same place in 1998. He is the author or co-author of more than 300 publications in his research fields including the book "*Control in Power Electronics*" (New York: Academic, 2002). He received the 1995 Angelos Award for his contribution in modulation technique and control of electric drives, and the Annual Teacher prize at Aalborg University in 1995. In 1998 he received the Outstanding Young Power Electronics Engineer Award from the IEEE Power Electronics Society. He has received four IEEE Prize paper awards during the last five years. In 2002 he received the C.Y.O'Connor fellowship from Perth, Australia, the Statoil-prize in 2003 for his contributions in Power Electronics, and the Grundfos-prize in 2004 for his contributions in power electronics and drives. He is associate editor of the IEEE Transactions on Industry Applications, IEEE Transactions on Power Electronics, Journal of Power Electronics and of the Danish journal Elteknik. He has held a number of chairman positions in research policy and research funding bodies in Denmark.